

## **UC Davis**

### **UC Davis Previously Published Works**

#### **Title**

CTC clusters induced by heparanase enhance breast cancer metastasis.

#### **Permalink**

<https://escholarship.org/uc/item/1z2844k5>

#### **Journal**

Acta Pharmacologica Sinica, 39(8)

#### **Authors**

Wei, Rong-Rui

Sun, Dan-Ni

Yang, Hong

et al.

#### **Publication Date**

2018-08-01

#### **DOI**

10.1038/aps.2017.189

Peer reviewed

## Article

# CTC clusters induced by heparanase enhance breast cancer metastasis

Rong-rui WEI<sup>1, #</sup>, Dan-ni SUN<sup>2, #</sup>, Hong YANG<sup>2</sup>, Juan YAN<sup>2</sup>, Xiong ZHANG<sup>2</sup>, Xing-ling ZHENG<sup>2</sup>, Xu-hong FU<sup>2</sup>, Mei-yu GENG<sup>2</sup>, Xun HUANG<sup>2, \*,</sup>, Jian DING<sup>2, \*</sup>

<sup>1</sup>Department of New Drug Screening Center, China Pharmaceutical University, Nanjing 210009, China; <sup>2</sup>Division of Anti-tumor Pharmacology, State Key Laboratory of Drug Research, Shanghai Institute of Materia Medica, Chinese Academy of Sciences, Shanghai 201203, China

### Abstract

Aggregated metastatic cancer cells, referred to as circulating tumor cell (CTC) clusters, are present in the blood of cancer patients and contribute to cancer metastasis. However, the origin of CTC clusters, especially intravascular aggregates, remains unknown. Here, we employ suspension culture methods to mimic CTC cluster formation in the circulation of breast cancer patients. CTC clusters generated using these methods exhibited an increased metastatic potential that was defined by the overexpression of heparanase (HPSE). Heparanase induced FAK- and ICAM-1-dependent cell adhesion, which promoted intravascular cell aggregation. Moreover, knockdown of heparanase or inhibition of its activity with JG6, a heparanase inhibitor, was sufficient to block the formation of cell clusters and suppress breast cancer metastasis. Our data reveal that heparanase-mediated cell adhesion is critical for metastasis mediated by intravascular CTC clusters. We also suggest that targeting the function of heparanase in cancer cell dissemination might limit metastatic progression.

**Keywords:** human breast cancer; CTC clusters; heparanase; metastasis; cell adhesion; adhesion molecules; suspension culture method

Acta Pharmacologica Sinica (2018) 39: 1326–1337; doi: 10.1038/aps.2017.189; published online 8 Feb 2018

### Introduction

Metastasis occurs when cancer cells migrate to and colonize a tissue microenvironment that is distant from the primary tumor<sup>[1]</sup>. This process occurs when malignant cells with migratory traits break off from primary tumors and disseminate through the circulation<sup>[2]</sup>. Circulating metastatic cell aggregates consisting of tumor cells have been reported in both clinical and mouse models<sup>[3, 4]</sup>. These circulating tumor cell (CTC) clusters have a much higher metastatic capability than single CTCs with identical genetic background<sup>[3, 5]</sup>. Moreover, the presence of CTC clusters in patients has been found to be associated with a poor prognosis.

The origins and integrity of CTC clusters are important for the heterogeneity of cancer metastases and are interesting to study. CTC clusters can arise directly from primary tumors or

form due to the aggregation of single CTCs. Based on the evidence from mouse models indicating the role of angiogenesis in this process, the intravascular aggregation of CTCs has been demonstrated as one of the mechanisms of formation of CTC clusters<sup>[6, 7]</sup>. In blood vessels, physical damage from hemodynamic shear forces exerts a selection pressure resulting in the death of malignant cells lacking adhesion by a process known as anoikis<sup>[8, 9]</sup>. Thus, CTC clusters in which strong cell-cell adhesions are preserved may have a survival advantage in the circulation and during dissemination. Single-cell sequencing of CTC clusters has revealed significant overexpression of junction components of either desmosomes or adherens junctions, which represent the two main types of cell-cell contacts. Plakoglobin and keratin 14<sup>[3, 10–12]</sup>, constituents of both adhesion junctions and desmosomes, are overexpressed in CTC clusters compared to their expression in matched single CTCs. These results indicate that certain factors involved in cell adhesion are likely to contribute to cancer metastasis. Heparanase (HPSE) is an endoglycosidase associated with metastasis<sup>[13, 14]</sup>. Importantly, heparanase is involved in cell adhesion by its non-enzymatic activity<sup>[15, 16]</sup>. Heparanase mediates the clustering of syndecan,

<sup>#</sup> These authors contributed equally to this work.

<sup>\*</sup> To whom correspondence should be addressed.

E-mail jding@simm.ac.cn (Jian DING);

xhuang@simm.ac.cn (Xun HUANG)

Received 2017-08-18 Accepted 2017-11-26

which is connected to the actin cytoskeleton, and can therefore contribute to cell adhesion<sup>[16]</sup>. Other adhesion molecules, such as  $\beta$ 1-integrin, ICAM-1, and VCAM have also been reported to participate in heparanase-induced cell adhesion and malignancy in a context-dependent manner<sup>[17, 18]</sup>. Heparanase is associated with metastasis and cell adhesion, but its role in CTCs and CTC clusters is still unknown.

In this study, we mimicked the aggregation of breast cancer cells in circulation via suspension culture methods and analyzed the metastatic characteristics of these cell clusters. We found that heparanase is associated with cell adhesion, and it promotes the formation of cell clusters. This role of heparanase had not been previously described in relation to cancer cell dissemination and is thus likely to increase our understanding of the function of heparanase in cancer metastasis.

## Materials and methods

### Cell lines

Human breast cancer cell lines MDA-MB-231, MDA-MB-468, HS578T and BT20 were purchased from American Type Culture Collection (Manassas, VA, USA). HCC1395 and BT-549 cells were obtained from the Cell Bank of the Chinese Academy of Sciences (Shanghai, China). Cell lines were authenticated by short tandem repeat analyses (Genesky Biotechnologies, Shanghai, China). Cells were maintained in appropriate culture medium suggested by the suppliers.

### Antibodies, reagents and inhibitors

Antibodies against heparanase and ICAM-1 were purchased from Santa Cruz Biotechnology (Santa Cruz, CA, USA). Antibodies against FAK, phospho-FAK (Y925), Src, phospho-Src (Y416), paxillin and phospho-paxillin (Y118) were purchased from Cell Signaling Technology (Beverly, MA, USA). CFDA SE (carboxyfluorescein diacetate) was purchased from Beyotime Institute of Biotechnology (Shanghai, China). *D*-Luciferin was purchased from Yeasen (Shanghai, China), dissolved in distilled water at 30 mg/mL to form a stock solution and diluted to a working solution at 15 mg/mL for animal experiments before use. PF-562271, KX2-391 and A-205804 were purchased from Selleck Chemicals (Houston, TX, USA). JG6 was synthesized and prepared in our lab.

### Two suspension culture methods for the formation of cell clusters

For the flask-based method, 4 mL of cell suspension ( $1 \times 10^5$  cells/mL) were seeded in flasks. The flasks were placed on a shaking table concentrator (37°C at 60 revolutions per minute), and the number of cell clusters formed was quantified after 6 h or 12 h.

For the circulating device-based method, a circulating device was attached to a sterile loop system, consisting of a peristaltic pump, silicone tube and 50 mL centrifuge tube, and placed in an incubator (37°C). Fifteen milliliters of cell suspension ( $1.5 \times 10^5$  cells/mL) were added to the 50 mL centrifuge tube, and the cell suspension was circulated through the tubing with the peristaltic pump. The number of cell clusters formed was quantified after 6 h or 12 h. The cell suspension (4 mL)

was transferred from the 50 mL centrifuge tube into a flask to facilitate the quantification of cell clusters.

Quantification method: With the flasks placed flat, five random fields were imaged with a microscope at 10 $\times$  magnification, and the average number of cell clusters in each field was counted. An aggregate of three or more cells was considered one cell cluster. In statistics, the cell clusters were in the range of 3 to 100 cells in the *in vitro* models.

### *In vivo* study using a lung metastasis mouse model

The animal experiments were performed according to the institutional ethical guidelines on animal care and approved by the Animal Care and Use Committee at Shanghai Institute of Materia Medica. Four to six-week-old female BALB/c *nu/nu* mice were obtained from Beijing Vital River Laboratory Animal Technology Co, Ltd. For the bioluminescence-based lung metastasis model, mice were injected into the lateral tail vein with luciferase-expressing MDA-MB-231 cells ( $1 \times 10^6$  cells/0.2 mL) prepared either as single cells or cell clusters. After 5 weeks, the mice were intraperitoneally injected with 150 mg/kg *D*-luciferin and anesthetized; lung metastatic foci were monitored via bioluminescence imaging with an IVIS Spectrum system (Caliper Corporation, MA, USA). Lungs were collected after the mice were sacrificed for further hematoxylin and eosin (H&E) staining and histological examination.

For the JG6 efficacy study, mice were injected into the lateral tail vein with aggregated MDA-MB-231 cells at  $1 \times 10^6$  cells/0.2 mL. One week after the implantation, the mice were randomly divided into three groups ( $n=6$ ) and orally administered with vehicle (control) or JG6 at 100 or 200 mg/kg per day for 3 weeks. Body weights were measured every three days. Lungs were collected after the mice were sacrificed for further H&E staining and histological examination.

### Modified blood smear assay to detect aggregated tumor cells in the blood

After the mice were anesthetized, cells suspensions stained with CFDA SE were injected into the inferior vena cava at  $2 \times 10^6$  cells/0.4 mL per mouse. Cardiac puncture was performed to collect a small amount of blood, following which the mice were sacrificed. The blood sample was dropped on a glass slide and covered with a coverslip to form a "smear". The slides were immediately examined via fluorescence and differential interference contrast (DIC) microscopy, and the number of single cells and aggregated cells were counted. An aggregate of two or more cells was considered one cell cluster.

### Establishment of CRISPR-Cas9-mediated cell lines with stable knockdown of heparanase

The gene-specific guideRNA sequences were designed with the CRISPR design tool from the Zhang laboratory (<http://crispr.mit.edu/>) with the following sequences: Heparanase\_#1, 5'-TGCGCAAGCACAGGACGTCG-3' and Heparanase\_#2, 5'-CTGGCCAAGGTACGAAGCTT-3'. The complementary oligos were cloned into LentiCRISPRv2 vectors.

Lentiviruses were generated using pMD2G and psPAX2 packaging vectors in 293T cells. In addition, we constructed an empty lentiviral control vector.

MDA-MB-231 cells seeded in 6-well plates were infected with viral supernatant. After 48 h, the cells were selected with 1 µg/mL puromycin. The selected cells were collected and seeded into 96-well plates (1 cell/well) for colony formation. The heparanase-stable knockout clones were verified by Western blotting and gene sequencing and used for further analysis.

#### Immunofluorescence microscopy

Cell clusters were generated by flask-based culture methods described earlier, and were grown on the glass coverslips, which were pretreated with Poly-L-Lysine for cell clusters attachment. After attaching to the glass coverslips, the cells were fixed with 4% paraformaldehyde, permeabilized with phosphate-buffered saline (PBS) containing 0.1% Triton X-100. After blocking with 3% bovine serum albumin (BSA) for 1 h, the cells were incubated with primary antibodies overnight. These cells were then washed three times with PBS, and incubated with Alexa Fluor 488 goat anti-mouse IgG (H+L), Alexa Fluor 594 goat anti-rabbit IgG (H+L), or Alexa Fluor 647 goat anti-mouse IgG (H+L) secondary antibodies. Images were captured using an Olympus Fluorview 1000 confocal microscope and processed using an FV1000 Viewer.

#### Western blotting

Cells were lysed, and the protein concentration was assessed using BCA protein assay reagent (Beyotime Institute of Biotechnology, Shanghai, China). Target proteins were analyzed via Western blotting with specific antibodies.

#### Total RNA extraction, cDNA preparation and quantitative RT-PCR

Total RNA was extracted using the Qiagen RNeasy Mini Kit (Qiagen, Germantown, MD, USA). cDNA samples were prepared using the ThermoScript RT-PCR synthesis kit (Invitrogen, Carlsbad, CA, USA). Real-time polymerase chain reaction (RT-PCR) was performed using an ABI ViiA7 Fast Real-time PCR System and SYBR Green PCR Master Mix according to the manufacturer's protocol (Applied Biosystems, Foster City, CA, USA). Relative expression level of genes was calculated using the  $2^{-\Delta\Delta CT}$  method. GAPDH was used as a housekeeping gene for normalization. The primers used for RT-PCR analysis are as follows: Heparanase: 5'-ATGCTCAGTTGCTCCTGGAC-3' and 5'-TAAGTGCACCCATTGATGA-3'; and GAPDH: 5'-CCAGC-CGAGCCACATCGCTC-3' and 5'-ATGAGCCCCAGCCTTCTC-CAT-3'.

#### RNA interference

RNA interference was performed with Lipofectamine RNAiMAX according to the manufacturer's instructions (Invitrogen, Carlsbad, CA, USA). The short interfering RNA (siRNA) sequences were synthesized by Shanghai GenePharma (Shanghai, China). The sequences (sense strand) are as follows: siFAK#1: 5'-GGGCAUCAUUCAGAAGAUATT-3'; siFAK#2: 5'-CAGGUGAAGAGCGAUUAUATT-3';

siFAK#3: 5'-GAACCUCGCAGUCAUUUAUTT-3'; siSrc#1: 5'-GGCUCCAGAUUGUCAACAATT-3'; siSrc#2: 5'-GCCUCUCAGUGUCUGACUUTT-3'; siSrc#3: 5'-UCGGCUCAUUGAAGACAAUTT-3'; siPaxillin#1: 5'-CCAACUGGAAACCACACAUTT-3'; siPaxillin#2: 5'-GUCUCUUGGAUGAACUGGATT-3'; SiPaxillin#3: 5'-CUUCUUCUGUGCACAGUGUTT-3'; siICAM-1#1: 5'-GCCCAAGUUGUUGGGCAUATT-3'; siICAM-1#2: 5'-GGUGAGGAGAGAUCACCAUTT-3'; and siICAM-1#3: 5'-CCUAUGGCAACGACUCCUUTT-3'.

#### Statistical analysis

The data were represented as the mean±SD. Statistical difference was analyzed using two-tailed Student's *t*-test or one-way analysis of variance. A *P* value of <0.05 was considered to be statistically significant.

## Results

### Cell clusters generated from suspension cultures have a greater metastatic potential

To explore the biological properties of cell aggregation, we used two methods to aggregate cells into clusters, namely, via suspension culturing in flasks or passing the cells through a circulating device (Figure 1A and 1B). Cell clusters were formed and maintained under both culture conditions, which mimic CTC clusters in blood. A previous study has suggested that plakoglobin is required for CTC cluster formation<sup>[11]</sup>. We thus used three independent siRNAs to knockdown plakoglobin in MDA-MB-231 cells (Figure 1C) and detected the ability of the cells to aggregate via the two culture methods described earlier (Figure 1D and 1E). As expected, aggregation was significantly decreased in cells depleted of plakoglobin along with a change in morphology (Supplementary Figure S1). Overall, the *in vitro* experimental system was suitable to address the properties of cell clusters.

To verify whether the cell clusters display malignant characteristics such as metastatic potential, we employed an experimental metastasis mouse model. Suspensions of clustered or single MDA-MB-231 cells were injected into mice. We immediately detected the transit of the cell clusters through the blood stream, and five weeks later, we detected the presence lung metastatic foci using bioluminescence (Figure 1F). The MDA-MB-231 cells were labeled with CFDA SE (carboxyfluorescein diacetate) to make them fluoresce green for easy monitoring. Then the stained cells were aggregated into clusters or left as single cells and injected into the inferior vena cava of mice. We detected the presence of the cell clusters in blood smears using fluorescence microscopy. We found that the mean percentage of cell clusters composed of two or more cells was higher in the group that was injected with aggregated cells than that injected with single cells (Figure 1G). We then generated MDA-MB-231 cells transfected with luciferase-expressing plasmid for ease of quantification. Suspensions of luciferase-expressing MDA-MB-231 cells in the form of clusters or single cells were injected into tail veins of mice. Five weeks later, bioluminescence imaging showed that the group

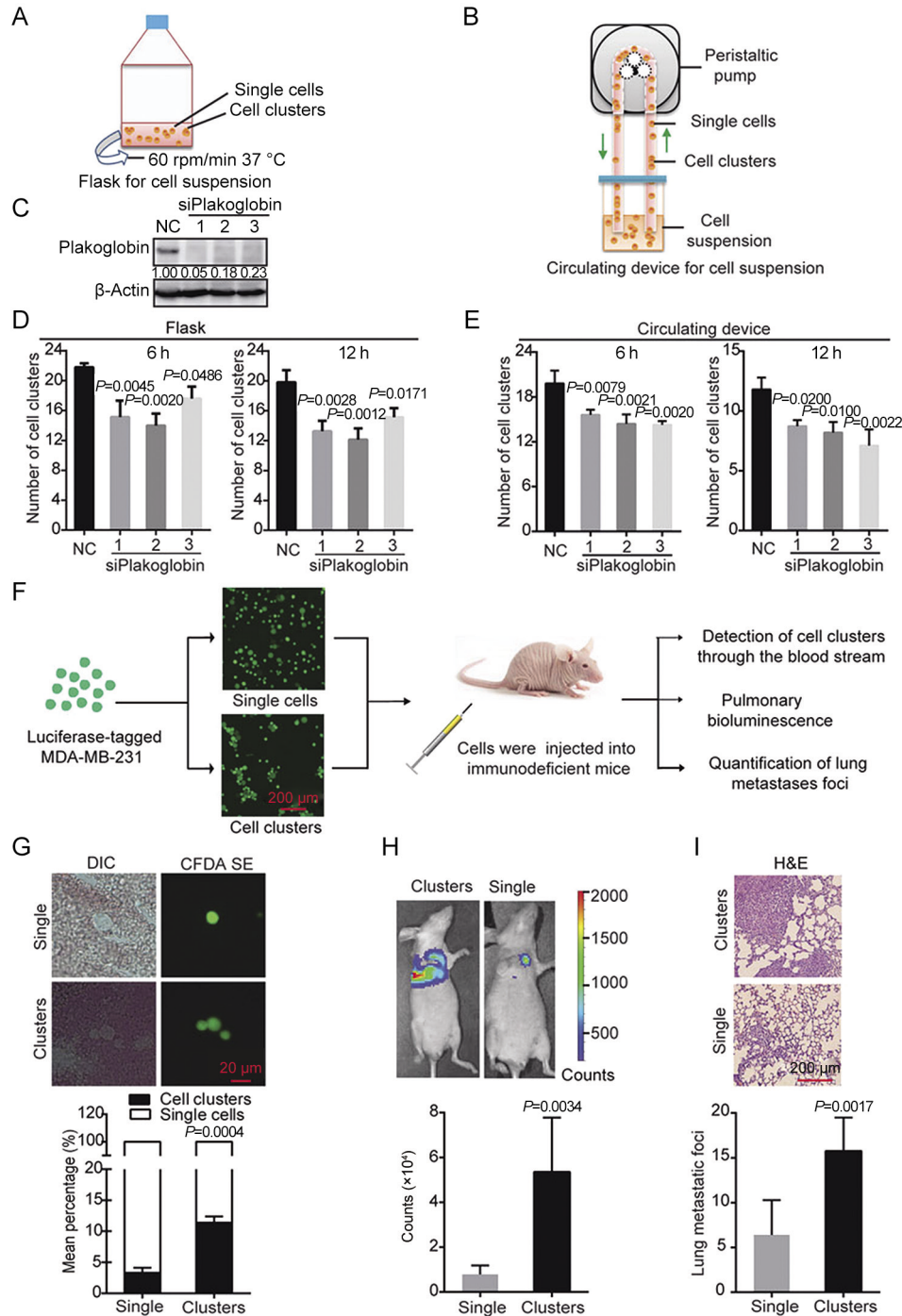


**Figure 1.** Cell clusters generated from suspension cultures have a greater metastatic potential. (A and B) Schematic of the experimental for cell clusters formation. (C) Knockdown efficiency of plakoglobin-specific siRNAs. MDA-MB-231 cells were transfected with non-targeting control (NC) or plakoglobin-specific siRNAs for 48 h followed by immunoblotting analysis. Densitometric data (fold) were shown. (D and E) The number of clusters formed by plakoglobin-depleted MDA-MB-231 cells in suspension culture for 6 h or 12 h using flasks or the circulating device. One-way ANOVA was applied in experiments containing multiple groups in (D) and (E). (F) The schema briefly explains the experimental lung metastasis model. Cells prepared as either single cells or clusters were injected into the tail vein of immunodeficient mice. Then, the status of tumor cells in the blood was immediately detected and the bioluminescence signals or lung metastatic foci were observed after 5 weeks. (G) Representative images of tumor cells from the blood using fluorescence and DIC microscopy. Histogram showing the mean percentage of single cells or cell clusters in groups injected with single cells or cell clusters. DIC, differential interference contrast. (H) Representative bioluminescence images of mice at 5 weeks after tail vein injection with luciferase-expressing MDA-MB-231 cells. Bar graph showing the quantification of bioluminescence signals in groups injected with single cells or cell clusters respectively. (I) Representative images of H&E-stained sections of mouse lungs in groups injected with single cells or cell clusters. Bar graph showing the number of lung metastatic foci in each group (n=6). Values are expressed as the mean±SD. Two tail student's t-test analysis was used to compare the statistical difference between indicated two groups in (G), (H), and (I).

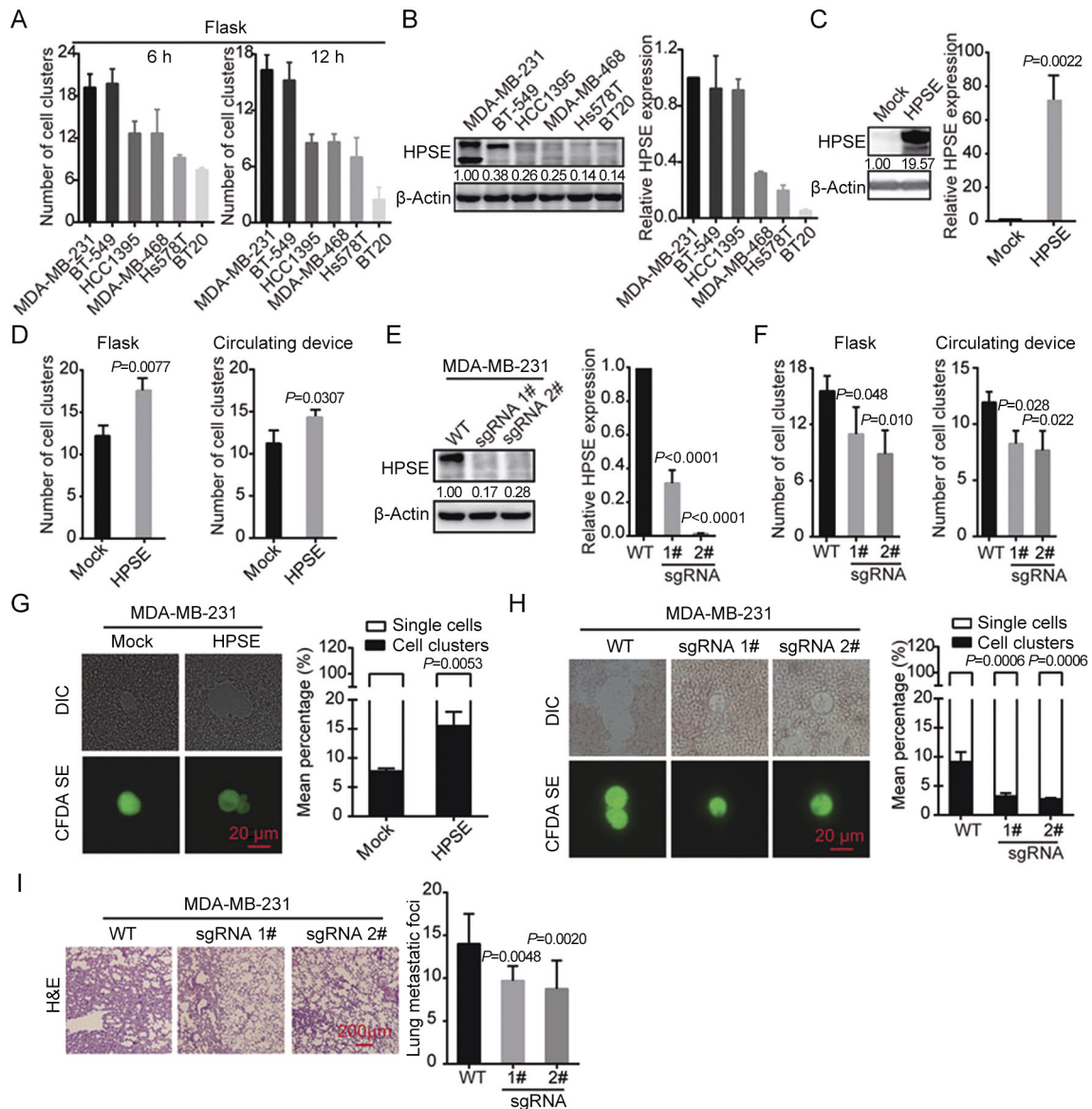


**Figure 2.** Heparanase promotes the formation of cell clusters and contributes to their metastatic potential. (A) Bar graph showing the number of cell clusters formed by six TNBC cell lines in suspended culture for 6 h or 12 h using flasks. (B) Heparanase expression was detected by immunoblotting and RT-PCR in different TNBC cell lines. Densitometric data (fold) were shown. (C) Immunoblotting and quantitative RT-PCR analysis of heparanase levels in MDA-MB-231 transfected with mock or heparanase-overexpression plasmid. Densitometric data (fold) were shown. (D) Histogram showing the number of heparanase-overexpressing MDA-MB-231 cell clusters in suspended culture for 12 h using flasks and a circulating device respectively. (E) Immunoblotting and quantitative RT-PCR analysis of heparanase knockout in MDA-MB-231 cells using CRISPR/Cas9 technology. Densitometric data (fold) were shown. (F) Histogram showing the number of heparanase-depleted MDA-MB-231 cell clusters in suspended culture for 12 h using flasks and a circulating device respectively. (G) Representative images of tumor cells from blood using fluorescence and DIC microscopy. Histogram showing the mean percentage of single cells or cell clusters in the groups transfected with mock or heparanase-overexpression plasmid. (H) Representative images of tumor cells from blood captured by fluorescence and DIC microscopy. Bar graph shows the percentage of single cells or cell clusters in the WT and heparanase-knockout groups. (I) Representative images of H&E-stained sections of mouse lungs in the WT and heparanase-knockout groups. Histogram showing the number of lung metastatic foci ( $n=6$ ). Values are expressed as the mean $\pm$ SD. Two tail Student's *t*-test analysis was used to compare the statistical difference between indicated two groups in (C), (D), and (G). One-way ANOVA was applied in experiments containing multiple groups in (E), (F), (H), and (I).

that was injected with aggregated cells had a higher metastatic burden than those injected with single cells (Figure 1H). In addition, H&E-stained sections of mouse lungs revealed that the cell clusters resulted in a higher number of metastatic foci, indicating more severe lung metastasis than the corresponding single cells (Figure 1I). These results indicate that cells aggre-

gated in clusters have a greater metastatic potential than that of single cells.

#### Heparanase promotes cluster formation and contributes to the metastatic potential of cells

Recently, CTCs have been shown to have prognostic sig-



nificance in patients with metastatic triple-negative breast cancer (TNBC) and have been associated with a higher risk of metastasis and progression<sup>[3, 19, 20]</sup>. We next assessed six TNBC cell lines using our experimental methods to probe cell cluster formation and found that MDA-MB-231 and BT549 cells had a higher cell clustering ability than the other cell lines (HCC1395, MDA-MB-468, HS578T and BT20) (Figure 2A, Supplementary Figure S2). We then investigated the mechanism underlying the differences in cell clusters formation in the various cell lines. Heparanase is an endoglycosidase that up-regulated in breast cancer and associated with elevated metastasis, advanced histological grade, and poor survival<sup>[21]</sup>. We hence detected heparanase expression in these cell lines. As expected, heparanase protein and mRNA expression were higher in the cell lines MDA-MB-231 and BT549 than other cell lines (Figure 2B). Thus, the ability of cell clustering was found to be positively correlated with the endogenous expression of heparanase.

To determine the correlation between heparanase and the ability of cells to aggregate, we derived heparanase-overexpressing MDA-MB-231 cells to evaluate the effect of heparanase on cell clustering based on the two methods described earlier (Figure 2C). The results revealed that heparanase-overexpressing MDA-MB-231 formed a higher number of cell clusters than control cells (Figure 2D). Meanwhile, we generated MDA-MB-231 cells with stable knockout of heparanase with the CRISPR/Cas9 technique (Figure 2E). As expected, heparanase-knockout MDA-MB-231 cells formed fewer clusters than the wild-type cells (Figure 2F). Thus, we confirmed the positive correlation between heparanase and cell cluster formation.

We then asked whether heparanase maintains the morphology of the cell clusters in the bloodstream where the cells are exposed to physical damage from hemodynamic shear forces. To this end, using the CFDA SE-stained blood smear assay, we detected the status of cell clusters from heparanase-overexpressing or heparanase-deficient MDA-MB-231 cells in the circulation of mice. Heparanase overexpression markedly increased the mean percentage of cell clusters in the blood, whereas heparanase knockout impaired cluster formation (Figure 2G and 2H). We next explored the role of heparanase in cell cluster-mediated lung metastasis using a mouse model. Heparanase-knockout MDA-MB-231 or WT MDA-MB-231 cells were injected into the tail vein of mice, and lung metastasis was assessed by counting the metastatic foci. Consistently, the number of metastatic foci in the heparanase knockout group was significantly lower than that in the WT group (Figure 2I). Taken together, these data demonstrate that heparanase promotes formation of clusters and thus contributes the metastatic potential of cells.

#### Heparanase increases the expression of adhesion molecules

The data presented in the present study have shown that heparanase promotes the formation of cell clusters. Previous studies have reported that heparanase facilitates tumor metastasis by altering cell-cell adhesion<sup>[17, 22]</sup>. FAK, Src<sup>[17, 23, 24]</sup>,

and ICAM-1<sup>[18]</sup> have been found to participate in heparanase-mediated cell adhesion and malignancy in a context-dependent manner. Hence, we asked whether heparanase regulates the expression of adhesion molecules. In heparanase-overexpressing MDA-MB-231 cells, we found that the phosphorylation of FAK, Src and paxillin and the expression of ICAM-1 were significantly elevated, whereas the protein level of FAK, Src, and paxillin was not affected (Figure 3A). Similar results were observed in BT-549 cells overexpressing heparanase (Supplementary Figure S3A). In contrast, the expression of ICAM-1 and the phosphorylation of FAK, Src, and paxillin were reduced in the heparanase-knockout MDA-MB-231 cells (Figure 3B). Taken together, these findings suggest that heparanase modulates the adhesion molecules FAK, Src, paxillin and ICAM-1. We then investigated whether these adhesion molecules existed in the cell clusters by an immunofluorescence assay, and MDA-MB-231 cell clusters were stained with FAK, paxillin and ICAM-1 antibody. Interestingly, we found there were more adhesion molecules in cell-cell contacts of the cell clusters (Figure 3C), similar results were observed in BT-549 cell clusters (Supplementary Figure S3B). These results suggested that heparanase contributes to cell cluster formation by modulating the adhesion molecules.

Although these adhesion molecules can be regulated by heparanase, the relationships among FAK, Src, paxillin and ICAM-1 are unclear. To further study these relationships, FAK inhibitor (PF-562271) and siRNAs were used to suppress the activity of FAK in MDA-MB-231 and BT549 cells. PF-562271 treatment and siRNA transfection successfully reduced FAK activity, and consequently suppressed the phosphorylation of FAK, Src, and paxillin in MDA-MB-231 and BT549 cells, whereas the expression of heparanase and ICAM-1 were not affected (Figure 3D, Supplementary Figure S3C). These results suggest that FAK and ICAM-1 are independent of each other. To further confirm these observations, ICAM-1 inhibitor (A-205804) and siRNAs were used to inhibit the expression of ICAM-1 in MDA-MB-231 and BT549 cells. A-205804 treatment and siRNA transfection successfully reduced ICAM-1 expression, whereas the expression of FAK, Src, paxillin and heparanase was not affected (Figure 3E, Supplementary Figure S3D). These data suggest that heparanase likely regulates the FAK-Src-paxillin pathway and the level of ICAM-1 through distinct mechanisms.

#### The ability of cells to aggregate was increased by adhesion molecules

From the above results, we found that heparanase increases the expression of adhesion molecules. We next determined whether the adhesion molecules FAK, Src, paxillin and ICAM-1 contribute to the formation of cell clusters. Thus, MDA-MB-231 cells were transfected with three independent siRNAs against FAK, Src, paxillin and ICAM-1 (Figure 4A), and the ability of the cells to aggregate was determined using the flask-based cell suspension culture method. We found that cell aggregation was significantly decreased when any of the four adhesion molecules was knocked down (Figure

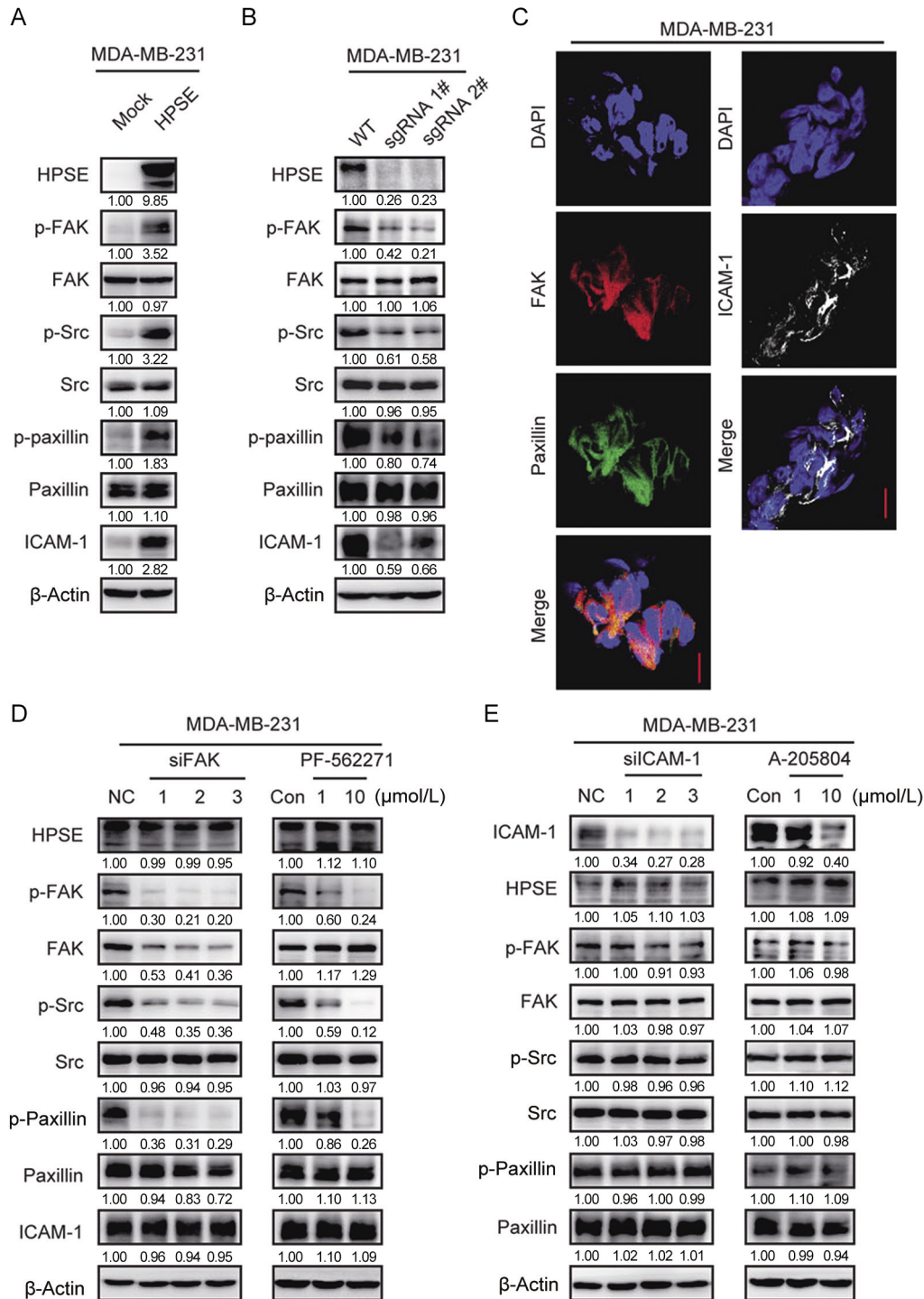


**Figure 3.** Heparanase increases the expression of adhesion molecules. (A) MDA-MB-231 cells stably transfected with mock or heparanase-overexpression plasmid were subjected to immunoblotting with indicated antibodies. (B) MDA-MB-231 cells depleted of heparanase using CRISPR/Cas9 technology were subjected to immunoblotting with the indicated antibodies. (C) Adhesion molecules localization. MDA-MB-231 cell clusters were stained for nuclei (blue), FAK (red), paxillin (green) or ICAM-1 (white) by immunofluorescence assay. Bar, 10  $\mu$ m. (D) MDA-MB-231 cells transfected with FAK-specific siRNAs or treated for 12 h with PF-562271 at the indicated concentrations were subjected to immunoblotting with indicated antibodies. (E) MDA-MB-231 cells transfected with ICAM-1-specific siRNAs or treated for 12 h with A-205804 at the indicated concentrations were subjected to immunoblotting with indicated antibodies. Densitometric data (fold) were shown below each group.

4B). These findings were confirmed with inhibitors against FAK, Src and ICAM-1. MDA-MB-231 cells were treated with PF-562271, KX2-391, or A-205804 at 1 or 10  $\mu$ mol/L for 12 h;

the phosphorylation level of FAK or Src or the expression of ICAM-1 was decreased (Figure 4C), and the number of cell clusters was decreased accordingly (Figure 4D). These data



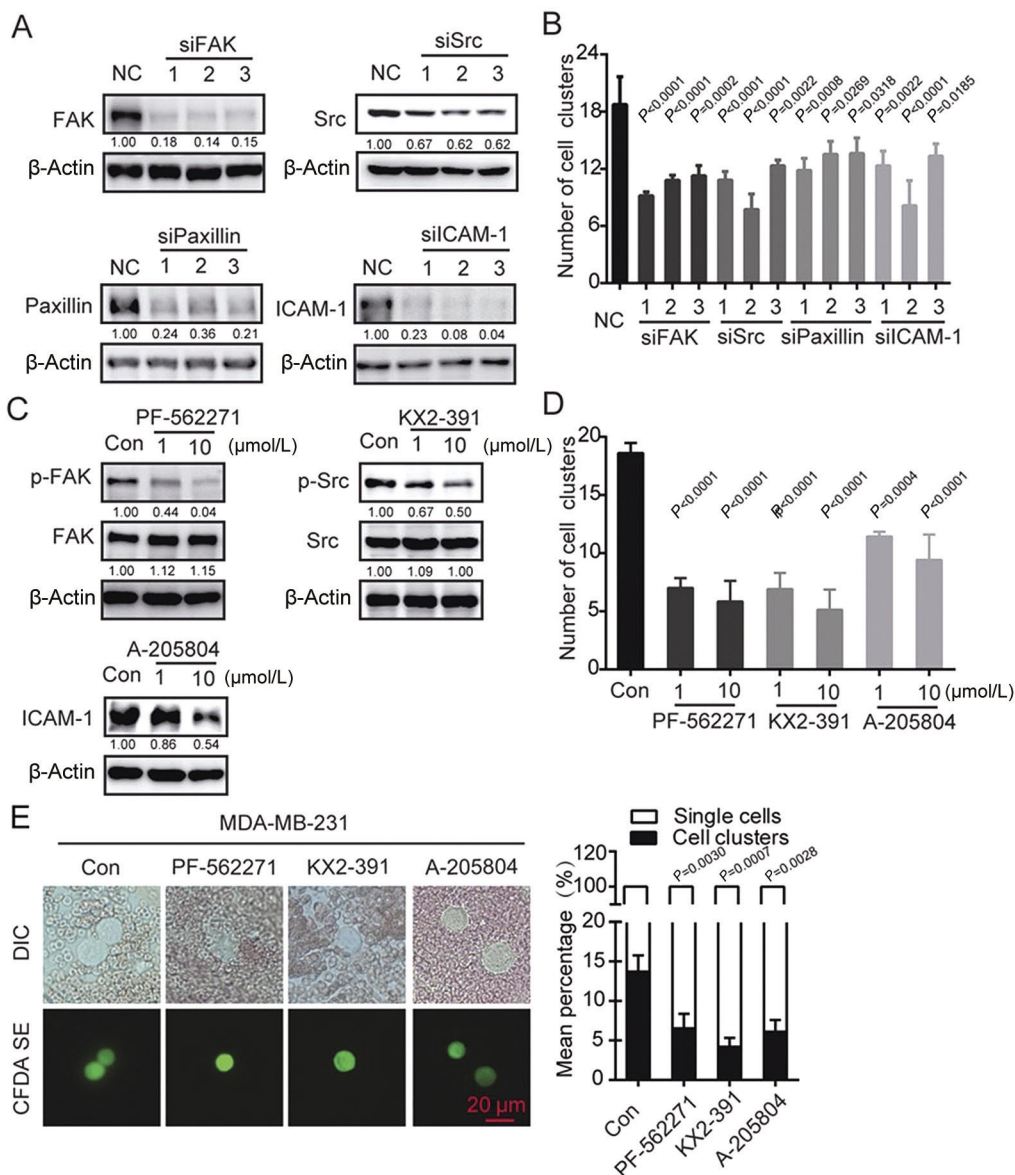


**Figure 4.** Cell aggregation was mediated by adhesion molecules. (A) MDA-MB-231 cells were transfected with siRNA against FAK, Src, paxillin or ICAM-1 followed by immunoblotting analysis. Densitometric data (fold) were shown below each group. (B) Bar graph showing the extent of aggregation of MDA-MB-231 cell suspensions cultured in flasks for 12 h after being transfected with siRNAs. One-way ANOVA was used to compare the statistical difference. (C) MDA-MB-231 cells were treated with PF-562271, KX2-391 or A-205804 for 12 h followed by immunoblotting analysis. Densitometric data (fold) were shown below each group. (D) Bar graph showing the extent of aggregation of MDA-MB-231 cells cultured in flasks for 12 h after treatment with the inhibitors. (E) Representative images of tumor cells from blood captured by fluorescence and DIC microscopy. The bar graph shows the mean percentage of single cells or cell clusters in the group of cells treated with inhibitor. Values are expressed as the mean±SD from three independent experiments. One-way ANOVA was used in experiments containing multiple groups in (D) and (E).

suggest that the four adhesion molecules, namely, FAK, Src, paxillin and ICAM-1 contribute to the formation of cell clusters. The results were further verified in animal experiments. MDA-MB-231 cells treated with PF-562271, KX2-391, or A-205840 for 12 h were prepared as suspensions and injected into mice. Morphological observation together with quantitative analysis of cell clusters showed that the inhibitor-treated cells displayed a marked decrease in the mean percentage of cell clusters in the blood (Figure 4E). These results suggest that the ability of cells to aggregate can be regulated by FAK,

Src, paxillin and ICAM-1.

#### Heparanase inhibitor JG6 decreases cell aggregation and the level of adhesion molecules

Our results above have demonstrated that heparanase induces the formation of cell clusters, which promotes metastasis. Previous studies have demonstrated the targeting of heparanase as a promising anti-metastasis strategy<sup>[25-27]</sup>. Additionally, heparanase inhibitors have been reported to produce good outcomes in clinical trials<sup>[28, 29]</sup>. Thus, we employed the hepa-

ranase inhibitor JG6, a novel marine-derived oligosaccharide, to determine the effect of heparanase on cell aggregation and the expression of adhesion-associated proteins. The  $IC_{50}$  value

of JG6 on heparanase activity was  $17.43 \mu\text{g/mL}$ , which was determined via the homogeneous time-resolved fluorescence assay (HTRF) (Figure 5A). To evaluate the effect of JG6 on cell

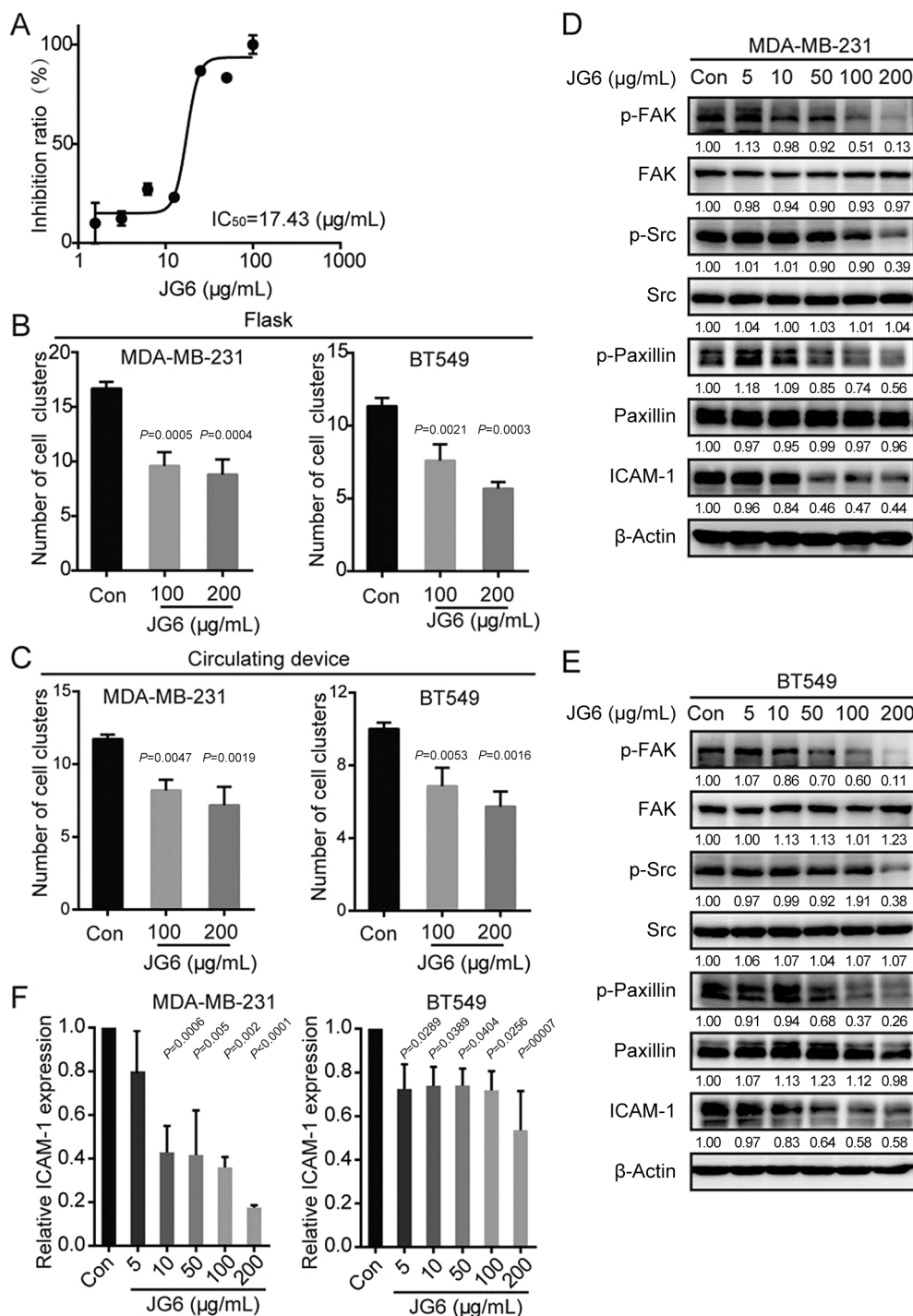


**Figure 5.** Heparanase inhibitor JG6 decreases the ability of cells aggregation and reduces the expression of adhesion molecules. (A) Dose-inhibition curve of JG6 examined by the HTRF assay. (B) The ability of MDA-MB-231 or BT549 cells to aggregate in flasks after treatment with the indicated concentrations of JG6 for 48 h. (C) The ability of MDA-MB-231 or BT549 cells to aggregate in the circulating device after treatment with the indicated concentrations of JG6 for 48 h. (D and E) MDA-MB-231 cells or BT549 cells were treated with various concentrations of JG6 for 48 h and subjected to immunoblotting with the indicated antibodies. Densitometric data (fold) were shown below each group. (F) Quantitative RT-PCR analysis of ICAM-1 levels in MDA-MB-231 or BT549 after being treated with the indicated concentrations of JG6 for 48 h. Values are expressed as the mean $\pm$ SD from three independent experiments. One-way ANOVA was applied in experiments containing multiple groups in (B), (C), and (F).

aggregation, MDA-MB-231 and BT549 cells were pre-treated with JG6 for 48 h and then subjected to cluster formation in the flask-based or circulating device-based method. JG6 pre-treatment inhibited cluster formation in MDA-MB-231 and BT-549 cells with both methods (Figure 5B and 5C). In addition, the phosphorylation of FAK, Src, and paxillin and the expression of ICAM-1 were reduced after JG6 treatment (Figure 5D–5F). These data demonstrate that JG6 reduced cell aggregation and down-regulated the expression of ICAM-1 and phosphorylation of FAK, Src and paxillin by inhibiting heparanase activity.

### Inhibition of heparanase with JG6 significantly blocks breast cancer metastasis *in vivo*

Our data thus far have demonstrated that heparanase promotes the formation of cell clusters, contributes to the metastatic potential of cells and regulates the expression of adhesion molecules but that these functions can be inhibited by the heparanase inhibitor JG6 *in vitro*. Because TNBC patients have poor clinical outcomes due to high rates of metastasis, we were interested to investigate the anti-metastatic effect of JG6 based on its inhibition of heparanase and subsequent reduction of cell cluster formation. To this end, MDA-MB-231 cells pre-treated with 100 or 200 µg/mL JG6 for 48 h were injected into the inferior vena cava of mice. The results showed that JG6 pre-treatment could significantly decrease the number of cell clusters in the mouse blood (Figure 6A). We next evaluated the anti-metastasis potential of JG6 using the cell cluster-

based experimental lung metastasis mouse model with MDA-MB-231 cells. One week after tumor cell inoculation, the mice were randomly assigned to the vehicle or JG6 group and gavaged daily with vehicle or 100 mg/kg or 200 mg/kg JG6, respectively, for 3 weeks. Lung metastasis was defined by the number of metastatic foci at the end point of the study. Compared with the vehicle, JG6 decreased the number of lung metastatic nodules in a dose-dependent manner (Figure 6B). JG6-treated mice survived throughout the duration of the experiment and showed no sign of toxicity or body weight loss (Supplementary Figure S4). Taken together, these results demonstrate the potential of JG6 in cancer therapy by hindering heparanase-mediated cell cluster formation and cancer metastasis.

### Discussion

Accumulating evidence has shown that CTC clusters have a greater propensity to form distal metastasis than single CTCs<sup>[3,30]</sup>. However, the molecular mechanism of CTC clusters formation is not fully understood. The study showed that heparanase promotes the formation of cell clusters that have a higher metastatic potential than single cells. Heparanase can influence cell cluster formation by regulating the FAK-Src-paxillin pathway and ICAM-1 expression. Furthermore, heparanase inhibitor reduces tumor metastasis.

Available technologies are primarily designed to capture CTC clusters and might fail to sort them in a reliable man-

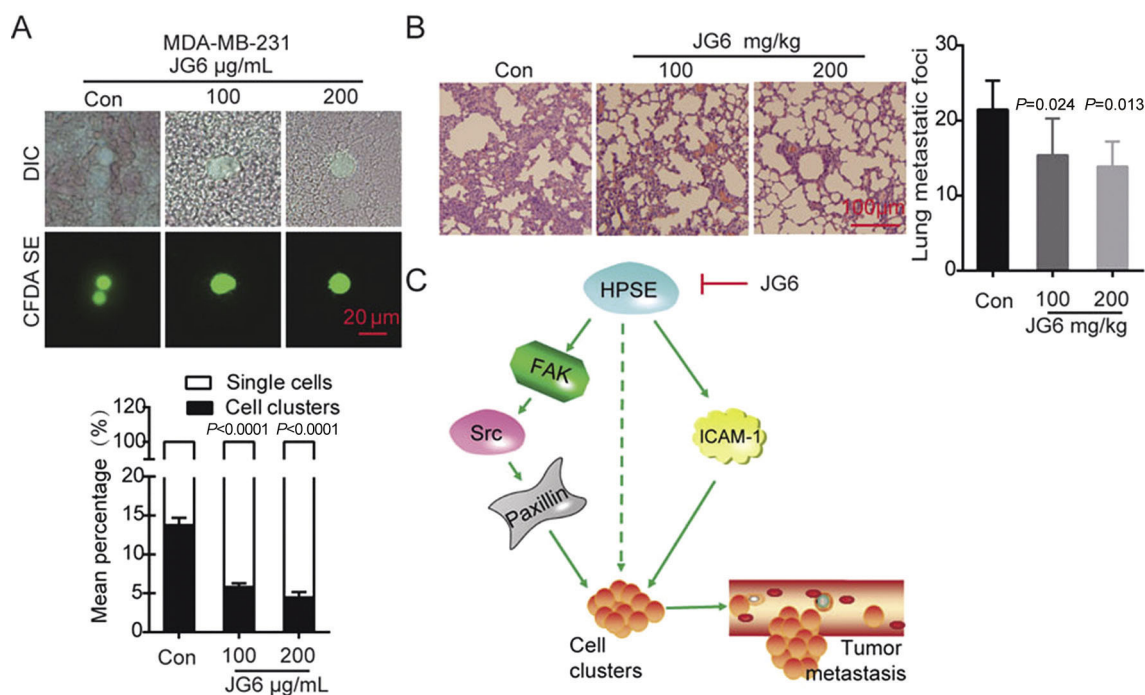


**Figure 6.** JG6 inhibits breast cancer metastasis. (A) MDA-MB-231 cells were treated with various concentrations of JG6 for 48 h and injected into the tail vein of mice. Shown were representative images of tumor cells in the blood captured by fluorescence and DIC microscopy. Bar graph showed the mean percentage of single cells or cell clusters in the groups, left untreated was served as control. (B) Representative images of H&E-stained sections of mouse lungs. Histogram showing the inhibitory effect of JG6 on the number of lung metastatic foci (n=6). (C) Proposed working model. Heparanase activates FAK-Src-paxillin and ICAM-1 signaling and promotes cell cluster formation, which increases tumor metastasis. JG6 inhibits this process induced by heparanase. Values are expressed as the mean±SD, One-way ANOVA was applied in experiments containing multiple groups in (A) and (B).

ner or to convey information on how these CTC clusters are formed. Aggregation of cells often occurs during cancer cell dissemination, and intravascular cell collision-mediated adhesion has been shown to be one mechanism of CTC cluster formation. Based on this knowledge, we introduced two suspension culture methods to mimic the vascular environment and study the formation and maintenance of CTC clusters. TNBC is known to be highly metastatic. Several recent studies have shown that the presence of CTC clusters is linked to TNBC metastasis and is regarded as a prognostic marker<sup>[12, 19, 31, 32]</sup>. In this study, six breast cancer cell lines were used in experiments to assess cell cluster formation, and the results showed that heparanase expression in TNBC cell lines, such as MDA-MB-231 and BT549, is positively associated with the ability of these cells to form clusters, which in turn is correlated with their metastatic potential<sup>[33]</sup>. Components of adherens junctions and desmosomes, such as plakoglobin and keratin 14, are critical for CTC clusters formation and promote distal metastases<sup>[3, 12]</sup>. Plakoglobin, a constituent of both adherens junctions and desmosomes, was knocked down in our study. As expected, the ability of cells to aggregate was significantly diminished with the depletion of plakoglobin. These data enabled the rational design of a CTC clustering method for further study.

A previous study has shown that adhesion molecules contribute to cellular aggregation. In a lung injury mouse model, the rapid induction of heparanase activity in pulmonary microvascular endothelial cells was shown to facilitate neutrophil recruitment through the elevation and presentation of cell adhesion molecules, such as ICAM-1 and VCAM-1, on endothelial cell surfaces<sup>[18]</sup>. Previous studies from our group and others have indicated that heparanase can mediate cell adhesion and dissemination through FAK and Src<sup>[17, 23, 24]</sup>. In the current study, we have found that heparanase knockout could reduce the expression of p-FAK, p-Src, p-paxillin and ICAM-1 and decrease the number of cell clusters. On the contrary, heparanase overexpression could increase the expression of p-FAK, p-Src, p-paxillin and ICAM-1 and the number of cell clusters. Moreover, knockdown of FAK, Src, paxillin and ICAM-1 by siRNAs or inhibitors decreased the number of cell clusters. The results suggest that heparanase influences cell aggregation by regulating the level of p-FAK, p-Src, p-paxillin and ICAM-1. In addition, auto-phosphorylation of FAK facilitates the interaction between FAK and Src, subsequently leading to the full activation of FAK via phosphorylation at other tyrosine sites<sup>[34, 35]</sup>. The activated FAK/SRC complex phosphorylates paxillin at Y118 to facilitate cell adhesion and migration<sup>[36]</sup>. In addition, ICAM-1 and FAK do not affect each other. Therefore, we conclude that heparanase mediates the aggregation of cells by regulating the FAK-Src-paxillin pathway and ICAM-1 expression. This study shows that heparanase regulates cell-cell adhesion, which plays an important role in CTC clusters formation.

Targeting heparanase can be a therapeutic strategy for preventing cancer metastasis, and heparanase inhibitors, such as PI-88, PG545, SST0001, have been reported<sup>[37]</sup>. In the study,

JG6, an inhibitor of heparanase, could inhibit the aggregation of cells *in vitro* or *in vivo* and suppress the FAK-Src-paxillin pathway and ICAM-1 expression. It could successfully decrease the number of lung metastatic foci in mice. Therefore, the therapeutic manipulations of CTC cluster formation can minimize tumor metastasis. Moreover, JG6 can decrease tumor metastasis by inhibiting heparanase. This study provides new insights into promising treatment strategies that may be able to reduce tumor metastasis based on the inhibition of CTC clustering via heparanase or related adhesion molecules. The therapeutic strategy of targeting heparanase to prevent cancer metastasis is highly promising.

### Acknowledgements

This work was supported by the National Natural Science Foundation of China (No 81302791), the Youth Innovation Promotion Association CAS, the Strategic Priority Research Program of the Chinese Academy of Sciences (No XDA12020326) and the Shanghai Talent Development Funds (No 201663), all awarded to Xun HUANG.

### Author contribution

Xun HUANG, Jian DING, and Mei-yu GENG designed research; Rong-rui WEI and Hong YANG performed research; Rong-rui WEI, Hong YANG, Juan YAN, Xiong ZHANG, Xingling ZHENG, and Xu-hong FU analyzed data; Xun HUANG, Rong-rui WEI, Dan-ni SUN, and Xiong ZHANG drafted the manuscript; Xun HUANG, Mei-yu GENG, and Jian DING provided supervision.

### Supplementary information

Supplementary information is available on the website of Acta Pharmacologica Sinica.

### References

- Hanahan D, Weinberg RA. Hallmarks of cancer: the next generation. *Cell* 2011; 144: 646–74.
- Massague J, Obenauf AC. Metastatic colonization by circulating tumour cells. *Nature* 2016; 529: 298–306.
- Aceto N, Bardia A, Miyamoto DT, Donaldson MC, Wittner BS, Spencer JA, et al. Circulating tumor cell clusters are oligoclonal precursors of breast cancer metastasis. *Cell* 2014; 158: 1110–22.
- Nguyen-Ngoc KV, Cheung KJ, Brenot A, Shamir ER, Gray RS, Hines WC, et al. ECM microenvironment regulates collective migration and local dissemination in normal and malignant mammary epithelium. *Proc Natl Acad Sci U S A* 2012; 109: E2595–604.
- Choi JW, Kim JK, Yang YJ, Kim P, Yoon KH, Yun SH. Urokinase exerts antimetastatic effects by dissociating clusters of circulating tumor cells. *Cancer Res* 2015; 75: 4474–82.
- Borsig L, Wong R, Hynes RO, Varki NM, Varki A. Synergistic effects of L- and P-selectin in facilitating tumor metastasis can involve non-mucin ligands and implicate leukocytes as enhancers of metastasis. *Proc Natl Acad Sci U S A* 2002; 99: 2193–8.
- Gasic GJ, Gasic TB, Galanti N, Johnson T, Murphy S. Platelet-tumor-cell interactions in mice. The role of platelets in the spread of malignant disease. *Int J Cancer* 1973; 11: 704–18.
- Hou JM, Krebs M, Ward T, Sloane R, Priest L, Hughes A, et al. Circulating tumor cells as a window on metastasis biology in lung

- cancer. *Am J Pathol* 2011; 178: 989–96.
- 9 Yu M, Bardia A, Wittner BS, Stott SL, Smas ME, Ting DT, et al. Circulating breast tumor cells exhibit dynamic changes in epithelial and mesenchymal composition. *Science* 2013; 339: 580–4.
  - 10 Fukunaga Y, Liu H, Shimizu M, Komiya S, Kawasuji M, Nagafuchi A. Defining the roles of beta-catenin and plakoglobin in cell-cell adhesion: isolation of beta-catenin/plakoglobin-deficient F9 cells. *Cell Struct Funct* 2005; 30: 25–34.
  - 11 Lu L, Zeng H, Gu X, Ma W. Circulating tumor cell clusters-associated gene plakoglobin and breast cancer survival. *Breast Cancer Res Treat* 2015; 151: 491–500.
  - 12 Cheung KJ, Padmanaban V, Silvestri V, Schipper K, Cohen JD, Fairchild AN, et al. Polyclonal breast cancer metastases arise from collective dissemination of keratin 14-expressing tumor cell clusters. *Proc Natl Acad Sci U S A* 2016; 113: E854–63.
  - 13 Vornicova O, Boyango I, Feld S, Naroditsky I, Kazarin O, Zohar Y, et al. The prognostic significance of heparanase expression in metastatic melanoma. *Oncotarget* 2016; 7: 74678–85.
  - 14 Ilan N, Elkin M, Vlodaysky I. Regulation, function and clinical significance of heparanase in cancer metastasis and angiogenesis. *Int J Biochem Cell B* 2006; 38: 2018–39.
  - 15 Goldshmidt O, Zcharia E, Cohen M, Aingorn H, Cohen I, Nadav L, et al. Heparanase mediates cell adhesion independent of its enzymatic activity. *FASEB J* 2003; 17: 1015–25.
  - 16 Levy-Adam F, Feld S, Suss-Toby E, Vlodaysky I, Ilan N. Heparanase facilitates cell adhesion and spreading by clustering of cell surface heparan sulfate proteoglycans. *PLoS One* 2008; 3: e2319.
  - 17 Zetser A, Bashenko Y, Miao HQ, Vlodaysky I, Ilan N. Heparanase affects adhesive and tumorigenic potential of human glioma cells. *Cancer Res* 2003; 63: 7733–41.
  - 18 Schmidt EP, Yang Y, Janssen WJ, Gandjeva A, Perez MJ, Barthel L, et al. The pulmonary endothelial glycocalyx regulates neutrophil adhesion and lung injury during experimental sepsis. *Nat Med* 2012; 18: 1217–23.
  - 19 Mu Z, Wang C, Ye Z, Austin L, Civan J, Hyslop T, et al. Prospective assessment of the prognostic value of circulating tumor cells and their clusters in patients with advanced-stage breast cancer. *Breast Cancer Res Treat* 2015; 154: 563–71.
  - 20 Magbanua MJM, Carey LA, DeLuca A, Hwang J, Scott JH, Rimawi MF, et al. Circulating tumor cell analysis in metastatic triple-negative breast cancers. *Clin Cancer Res* 2015; 21: 1098–105.
  - 21 Sun X, Zhang G, Nian J, Yu M, Chen S, Zhang Y, et al. Elevated heparanase expression is associated with poor prognosis in breast cancer: a study based on systematic review and TCGA data. *Oncotarget* 2017; 8: 43521–35.
  - 22 Levy-Adam F, Ilan N, Vlodaysky I. Tumorigenic and adhesive properties of heparanase. *Semin Cancer Biol* 2010; 20: 153–60.
  - 23 Li QN, Liu HY, Xin XL, Pan QM, Wang L, Zhang J, et al. Marine-derived oligosaccharide sulfate (JG3) suppresses heparanase-driven cell adhesion events in heparanase over-expressing CHO-K1 cells. *Acta Pharmacol Sin* 2009; 30: 1033–8.
  - 24 Reiland J, Kempf D, Roy M, Denkins Y, Marchetti D. FGF2 binding, signaling, and angiogenesis are modulated by heparanase in metastatic melanoma cells. *Neoplasia* 2006; 8: 596–606.
  - 25 Zhao HJ, Liu HY, Chen Y, Xin XL, Li J, Hou YT, et al. Oligomannurate sulfate, a novel heparanase inhibitor simultaneously targeting basic fibroblast growth factor, combats tumor angiogenesis and metastasis. *Cancer Res* 2006; 66: 8779–87.
  - 26 Khamaysi I, Singh P, Nasser S, Awad H, Chowders Y, Sabo E, et al. The role of heparanase in the pathogenesis of acute pancreatitis: a potential therapeutic target. *Sci Rep-Uk* 2017; 7: 715.
  - 27 Sanderson RD, Elkin M, Rapraeger AC, Ilan N, Vlodaysky I. Heparanase regulation of cancer, autophagy and inflammation: new mechanisms and targets for therapy. *FEBS J* 2017; 284: 42–55.
  - 28 Liu CJ, Chang J, Lee PH, Lin DY, Wu CC, Jeng LB, et al. Adjuvant heparanase inhibitor PI-88 therapy for hepatocellular carcinoma recurrence. *World J Gastroenterol* 2014; 20: 11384–93.
  - 29 Lewis KD, Robinson WA, Millward MJ, Powell A, Price TJ, Thomson DB, et al. A phase II study of the heparanase inhibitor PI-88 in patients with advanced melanoma. *Invest New Drug* 2008; 26: 89–94.
  - 30 Hou JM, Krebs MG, Lancashire L, Sloane R, Backen A, Swain RK, et al. Clinical significance and molecular characteristics of circulating tumor cells and circulating tumor microemboli in patients with small-cell lung cancer. *J Clin Oncol* 2012; 30: 525–32.
  - 31 Jansson S, Bendahl PO, Larsson AM, Aaltonen KE, Ryden L. Prognostic impact of circulating tumor cell apoptosis and clusters in serial blood samples from patients with metastatic breast cancer in a prospective observational cohort. *BMC Cancer* 2016; 16: 433.
  - 32 Wang C, Mu Z, Chervoneva I, Austin L, Ye Z, Rossi G, et al. Longitudinally collected CTCs and CTC-clusters and clinical outcomes of metastatic breast cancer. *Breast Cancer Res Treat* 2017; 161: 83–94.
  - 33 Fabisiewicz A, Grzybowska E. CTC clusters in cancer progression and metastasis. *Med Oncol* 2017; 34: 12.
  - 34 Mitra SK, Hanson DA, Schlaepfer DD. Focal adhesion kinase: in command and control of cell motility. *Nat Rev Mol Cell Biol* 2005; 6: 56–68.
  - 35 Zhao X, Guan JL. Focal adhesion kinase and its signaling pathways in cell migration and angiogenesis. *Adv Drug Deliv Rev* 2011; 63: 610–5.
  - 36 Luo M, Guan JL. Focal adhesion kinase: a prominent determinant in breast cancer initiation, progression and metastasis. *Cancer Lett* 2010; 289: 127–39.
  - 37 Jia L, Ma S. Recent advances in the discovery of heparanase inhibitors as anti-cancer agents. *Eur J Med Chem* 2016; 121: 209–20.